Biomaterials 31 (2010) 6087–6095

Contents lists available at ScienceDirect

Biomaterials

journal homepage: www.elsevier.com/locate/biomaterials

An optical biosensing platform for proteinase activity using gold nanoparticles

Yao-Chen Chuang, Jung-Chun Li, Sz-Hau Chen, Ting-Yu Liu, Ching-Han Kuo, Wei-Ting Huang, Chih-Sheng Lin*

Department of Biological Science and Technology, National Chiao Tung University, Hsinchu 30068, Taiwan

ARTICLE INFO

Article history:
Received 3 February 2010
Accepted 12 April 2010
Available online 14 May 2010

Keywords:
6-Mercaptohexan-1-ol
Gold nanoparticles
Matrix metalloproteinase
Optical biosensor
Proteinase

ABSTRACT

The surface plasmon resonance (SPR) wavelength of colloidal gold nanoparticles (AuNPs) can vary when the AuNPs aggregate, have different sizes or shapes, or are modified with chemical molecules. In this study, an optical biosensing platform for a proteinase activity assay was established based on the SPR property of AuNPs. The 13-nm AuNPs were modified with gelatin (AuNPs-gelatin) as a proteinase substrate and subsequently modified with 6-mercaptohexan-1-ol (MCH) (AuNPs/MCH-gelatin). After proteinase (trypsin or gelatinase) digestion, the AuNPs lose shelter, and MCH increases the attractive force between the modified AuNPs. Therefore, the AuNPs gradually move closer to each other, resulting in AuNPs aggregation. The AuNPs aggregation can be monitored by the red shift of surface plasmon absorption and a visible color change of the AuNPs is from red to blue. Such a color change can be observed with the naked eye. For detection, the absorption ratio, A_{625}/A_{525}, of the reacted AuNPs solution can be used to estimate quantitatively the proteinase activity. A linear correlation has been established with trypsin activity at concentrations from 1.25×10^{-1} to 1.25×10^{2} U and matrix metalloproteinase-2 activity at concentrations from 50 ng/mL to 600 ng/mL.

1. Introduction

The degradation of substrates by proteinase plays an important role in most metabolic and pathophysiological pathways. For example, a family of zinc-dependent proteinases, matrix metalloproteinases (MMPs), play key roles in several biological processes, including cell proliferation and migration, inflammation, and tissue remodeling [1,2]. In particular, because of their significant role in promoting cancer processes and cardiac disease [2–5], MMPs have become important targets for clinical tumor and heart disease diagnosis. Therefore, a sensitive and convenient assay for specific proteinase activity is needed for application to clinical diagnosis. Standard assays for proteinase activity include those based on substrate zymography, radioisotopes, or fluorogenic substrates. However, these techniques are time-consuming and require specific instrumentation; furthermore, labeled-substrates are expensive and inconvenient. Therefore a label-free and convenient method should be established for the assays of proteinase.

Nanoparticles, special gold nanoparticles (AuNPs), are the materials of interest in a rapidly developing area of biosensor [6–8]. AuNPs exhibit strong surface plasmon resonance (SPR) that depends on the size of AuNPs and the relative distance between AuNPs [9–11]. A colorimetric assay using the aggregation of AuNPs is a simple and sensitive method that can be used to detect biomolecules such as proteins, nucleic acids, enzymes, and cells [12–15]. Spherical AuNPs with an interparticle distance larger than the average particle diameter appears red in color. These particles' color can change from red to blue when the interparticle distance becomes smaller than the average particle diameter due to aggregation [16,17].

Currently, most of the AuNPs-based colorimetric assays for nucleic acids and enzymes detection are mainly dependent on the properties of enzyme catalysis, DNA hybridization [18,19], antigen–antibody reaction [20,21] and molecule interactions (such as protein–ligand interaction) [22–24] to induce a change in the AuNPs dispersion or AuNPs aggregation. Most of the AuNPs-based diagnoses using detection of enzyme activity are mainly dependent on enzyme catalysis to induce the change in AuNPs aggregation [25,26]. However, the use of AuNPs to establish a platform for the detection of enzyme activity faces some difficulties. The colloidal stabilization/aggregation phenomena of functionalized-AuNPs are rather complicated. For example, the charge and structure of proteins must be considered when discussing the stabilization/aggregation of protein-modified AuNPs. Additionally, the ion concentration in the reaction solution can affect enzyme activity

* Corresponding author. Department of Biological Science and Technology, National Chiao Tung University, No.75 Po-Ai Street, Hsinchu 30068, Taiwan. Tel.: +886 3 5131338; fax: +886 3 5729288.
E-mail address: lincs@mail.nctu.edu.tw (C.-S. Lin).

0142-9612/$ – see front matter © 2010 Elsevier Ltd. All rights reserved.
doi:10.1016/j.biomaterials.2010.04.026

and AuNPs stability. Therefore, in applying an AuNPs-based biosensing platform for the detection of enzyme activity, the modification process could promote monodispersed AuNPs to aggregate, in addition to the cations, which are supplied by the reaction buffer could also induce the aggregation of AuNPs.

It has been reported that macromolecules can be grafted onto the surfaces of colloidal AuNPs [27,28]. In this research, macromolecules were functionalized onto the AuNPs as the substrate and also provided a steric repulsion effect to prevent the AuNPs from coming into close contact [28,29]. Although the macromolecules protected the AuNPs stability, they also lowered the sensitivity of the AuNPs-based sensing methods. To overcome these serious problems, we have designed an AuNPs-based platform to assay the proteinase activity. In the present study, a biomolecule element was modified onto the AuNPs as a substrate, which kept the modified AuNPs stably suspended in solution. In addition, molecules of 6-mercaptohexan-1-ol (MCH) were modified on the AuNPs and played a role as an "inducer" to increase the attraction among the AuNPs. MCH served not only to block the surface space to avoid peptide absorption on the AuNPs but also to increase the attraction among the AuNPs. With the MCH modification, the AuNPs-based biosensing platform is more efficient when applied in an enzymatic assay of proteinase activity.

2. Experimental section

2.1. Chemicals

Sodium citrate was obtained from Merck (Darmstadt, Germany). Tris–HCl was purchased from Chemicon (Invitrogen, San Diego, LA, USA). Agarose and 10× Tris–Borate–EDTA buffer were purchased from Amresco (Cleveland, OH, USA). Sodium chloride (NaCl), calcium chloride ($CaCl_2$), MCH, Triton X-100, Tris–HCl, type A gelatin and hydrogen tetrachloroaurate (III) ($HAuCl_4 \cdot 3H_2O$) were purchased from Sigma–Aldrich (St. Louis, MO, USA). Trypsin, MMP-2, MMP-7 and MMP-9 were purchased from Sigma–Aldrich and MMP-1 was purchased from ProSpec (Rehovot, Israel). All chemicals were of analytical grade. Nanopure water was obtained by passing twice-distilled water through a Milli-Q system (18 MΩ cm; Millipore, Bedford, MA, USA).

2.2. Synthesis and modification of AuNPs

AuNPs were prepared by citrate reduction of $HAuCl_4 \cdot 3H_2O$ according to the reported procedure [30]. A 50 mL aqueous solution consisting of 2.5 mM $HAuCl_4 \cdot 3H_2O$ was brought to a vigorous boil with stirring in a conical flask, and then 38.8 mM trisodium citrate (5 mL) was added rapidly to the solution. The solution was boiled for another 15 min, during which time its color changed from pale yellow to deep red. The solution was cooled to room temperature with continuous stirring. The sizes of the AuNPs were verified by scanning electron microscope (SEM) (JEOL JEM 100 CX electron microscope; JEOL, Tokyo, Japan) and dynamic light scattering (DLS) (BI-200SM; Brookhaven Instruments, Holtsville, NY, USA). Citrate-stabilized AuNPs appeared to be nearly monodisperse, with an average size of 13 ± 1.2 nm. A UV–vis absorption spectrophotometer (Apices Scientific, Boston, MA, USA) was used to measure the absorbance of AuNPs in citrate solutions [8].

2.3. Modification of AuNPs

The modification process for adding gelatin and MCH to the AuNPs was monitored by observing the spectral changes after the addition of gelatin and MCH. The gelatin and MCH were modified onto the AuNP surfaces according to the following procedures. For the preparation of gelatin-modified AuNPs (addressed as AuNPs-gelatin), an aliquot of the aqueous AuNPs solution (950 μL) was mixed with an aqueous gelatin solution (0.1%, 50 μL) and incubated at 37 °C for 2 h. The mixture was then centrifuged for 6 min at 14,000 × *g* to remove the excess gelatin. After two centrifuge/wash cycles, the colloidal AuNPs-gelatin was resuspended in 200 μL NTTC buffer (50 mM NaCl, 50 mM Tris–HCl pH 7.5, 5 μM $CaCl_2$, and 0.05% triton X-100). To prepare gelatin and MCH-modified AuNPs (addressed as AuNPs/MCH-gelatin), AuNPs solution (950 μL) mixed with gelatin (0.1%, 50 μL) was incubated at 37 °C for 2 h, and then MCH (10 μL, 1 mM) was added to the solution and incubated at 37 °C for another 2 h. The mixture was then centrifuged for 6 min at 14,000 × *g* to remove the excess gelatin and MCH. After two centrifuge/wash cycles, the AuNPs/MCH-gelatin colloid was resuspended in 200 μL NTTC buffer. The concentration of modified AuNPs was adjusted to 5 nM for further use in the proteinase activity assay.

2.4. Proteinase activity assay by gelatin-modified AuNPs

For the proteinase activity assay, 50 μL trypsin or MMPs (including MMP-1, MMP-2, MMP-7 and MMP-9) of varying concentration was added into 200 μL of gelatin-modified AuNPs, and the mixture was incubated at 37 °C. All of the solutions were analyzed with UV–vis absorption spectrophotometer, which recorded their spectral profiles and calculated the ratios of absorbance at 625 and 525 nm (A_{625}/A_{525}) after a 10 min reaction time for trypsin and a 30 min reaction time for MMPs.

2.5. MMPs activity assay by zymography

The MMPs activity assay was also performed according to our previously described zymography method [8]. Briefly, MMPs were activated by APMA and then mixed with 2× zymography sample buffer (0.125 M Tris–HCl, pH 6.8, 20% (v/v) glycerol, 4% (w/v) SDS, and 0.005% bromophenol blue), incubated for 10 min at room temperature, and loaded into each lane of a SDS-PAGE (10%) gel containing 0.1 mg/mL gelatin. After electrophoresis, the gel was washed twice for 30 min in zymogram renaturing buffer (2.5% Triton X-100) with gentle agitation at room temperature to remove SDS, and then incubated at 37 °C for 8 h in reaction buffer (50 mM Tris–HCl, pH 7.4, 200 mM NaCl, and 5 mM $CaCl_2$). After staining with Coomassie brilliant blue, gelatinase activities were identified as clear zones against a blue background.

2.6. Electrophoresis analysis of gelatin-modified AuNPs

Gel electrophoresis analysis modified from Hanauer' protocol [31] was used to check the change in diameter of gelatin-modified AuNPs after proteinase digestion. Agarose gels were prepared with and immersed in 0.5× TBE buffer (Tris–Borate–EDTA buffer, prepared by diluting 10× stock solutions). Before loading the gels with the gelatin-modified AuNPs samples, the gelatin-modified AuNPs were mixed with sodium dodecyl sulfate (SDS), which imparts a negative charge on the gelatin coating of the AuNPs and causes them to run towards the positive electrode [32]. After proteinase digestion for 10 min, each sample of enzyme-treated AuNPs was loaded into one well of the gel. The gels were run in a horizontal electrophoresis system (Mini-Sub Cell GT; Biorad, Corston, UK) for 30 min at 110 V in 0.5× TBE buffer, followed by staining with Coomassie brilliant blue solution for 30 min. Finally, the gel was destained with destaining buffer. After electrophoresis, gel images were taken with a digital camera and processed with only small linear contrast adjustments in order to obtain a true representation of the visual gel appearance.

2.7. Assay of trypsin and MMPs activity by SDS-PAGE

The gelatin digestion activities of trypsin, MMP-1, MMP-2, MMP-7 and MMP-9 were assayed. One microliter of proteinase (100 μg/mL) was added into 20 μL of 0.1% gelatin solution containing 50 mM NaCl, 50 mM Tris–HCl pH 7.5, 5 μM $CaCl_2$, and 0.05% Triton X-100, and the assay mixture was further incubated at 37 °C for 1 h. The final pH of the assay mixtures was 7.5. Following incubation, the assay mixture was heated at 95 °C for 10 min in the presence of electrophoresis sample buffer and subjected to 8% sodium dodecyl sulfate-polyacrylamide gel electrophoresis (SDS-PAGE). Proteins were stained with Coomassie brilliant blue R-250.

3. Results and discussion

3.1. Establishment of a colorimetric biosensing platform using AuNPs

AuNPs has been extensively applied in colorimetric biosensing methods for the detection of specific proteins and nucleic acids. Here, we have designed a simple proteinase colorimetric method using functionalized-AuNPs based on the optical property that causes the dispersed AuNPs solution to appear red in color, whereas the aggregated AuNPs solution appears as purple (or black).

Scheme 1 outlines the principal design of functionalized-AuNPs with/without the MCH modification used to assay the proteinase activity. MCH, containing a thiol group (−SH) and a hydroxyl group (−OH), plays an important role as an inducer in the development of the biosensing method. The molecules of MCH connect to the AuNPs through −SH substitution and the −OH exposed on AuNPs surface enhances the attraction force among AuNPs [8,18]. In addition, MCH molecules on the AuNPs also play a role as blockers [33]. MCH molecules cover the surface area of the AuNPs that are not conjugated with gelatin, and therefore the digested peptide will not adsorb on the AuNPs. For the proteinase assay, gelatin was modified onto AuNPs to generate AuNPs-gelatin. After that, AuNPs-gelatin was modified with MCH to produce AuNPs/MCH-gelatin.

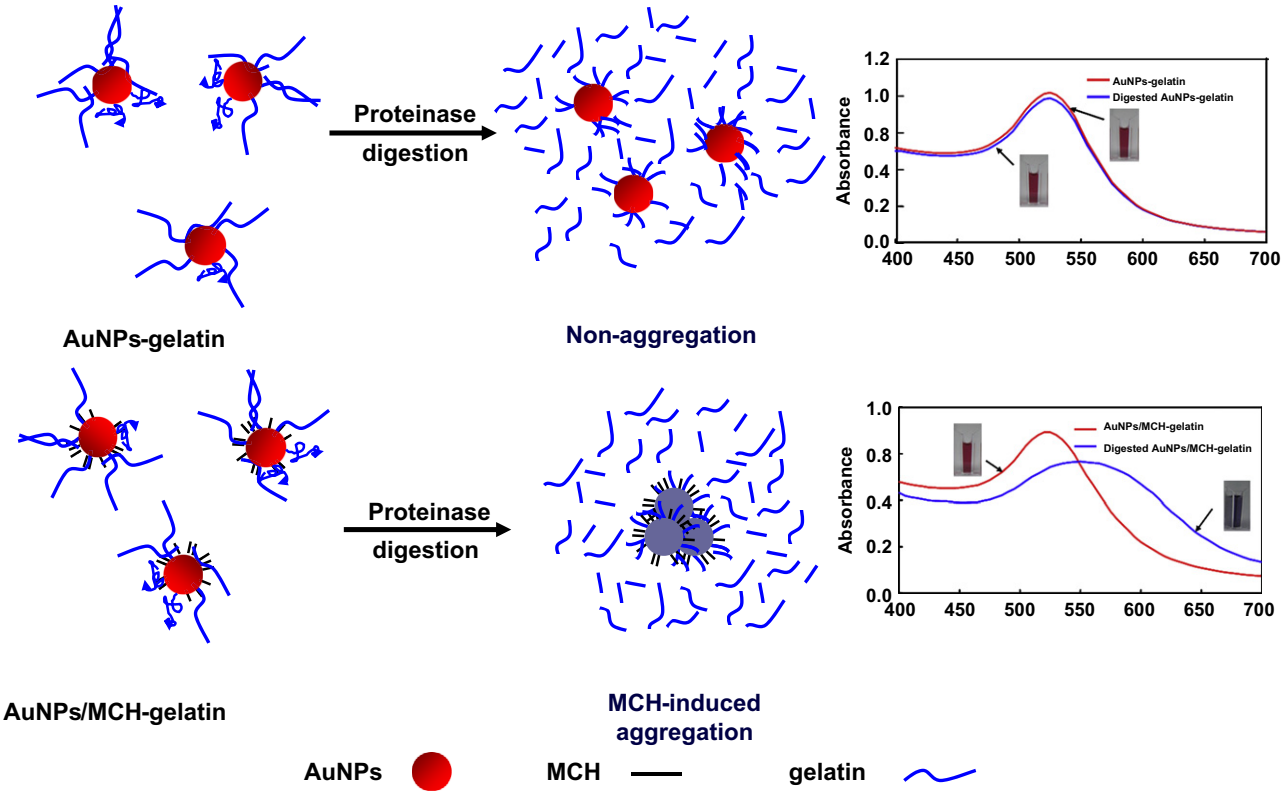

Scheme 1. Schematic illustration of the AuNPs-based optical biosensing platform used to assay proteinase activity. The AuNPs were functionalized with gelatin and without/with 6-mercaptohexan-1-ol (MCH) (as AuNPs-gelatin and AuNPs/MCH-gelatin, respectively). Before enzymatic digestion, both modified AuNPs were stable due to steric stabilization. During AuNPs-gelatin digestion by proteinase, AuNPs-gelatin stayed suspended in the reaction solution. However, the removal of gelatin (colloidal stabilizer) on the AuNP/MCH-gelatin surface by proteinase cleavage destabilized the AuNPs and resulted in nanoparticle aggregation (higher panel). Aggregation of AuNPs/MCH-gelatin results in a color change from pink red to violet blue (lower panel). The MCH molecule applied in this AuNPs platform plays dual roles as inducer and blocker, as proposed in Results and discussion section.

Both of the functionalized-AuNPs displayed the wine-red color. Upon enzymatic degradation of AuNPs-gelatin, the AuNPs underwent disassembly, and no detectable color change or spectrum shift occurred (Scheme 1; higher panel), i.e., the suspensions were stable without showing signs of aggregation. On the other hand, when proteinase acted to digest the AuNPs/MCH-gelatin, a significant color change from red to purple occurred within minutes. Both a decreased absorbance at 525 nm and an increased absorbance at 625 nm were observed in the UV–vis spectrum as time increased (Scheme 1; lower panel). The change of spectral profile indicated that the AuNPs became aggregated after proteinase digestion.

3.2. UV–Vis absorption spectrum of gelatin and MCH-modified AuNPs

Monitoring of the modification process can be done by direct observation of the surface plasmon resonance shift. In previous reports, the optical spectrum was used to estimate the particle sizes of the AuNPs, and the maximum absorbance (λ_{max}) of 13 nm AuNPs was located at 520 nm [34,35]. The typical UV–vis absorption of AuNPs-gelatin during the modification process is shown in Fig. 1. In Fig. 1A, the red-colored AuNPs (13 nm in diameter) displays an intense SPR absorption located at 520 nm. The UV–vis SPR peak shifts from 520 to 525 nm, and a slight increase in the intensity of the 525 nm peak occurs after the AuNPs were modified with gelatin [36]. In addition, a significant increasing absorption wavelength at 280 nm indicates the existence of gelatin on the AuNPs surface, as evidenced by the functional groups of amino acids in the UV–vis spectrum [37]. Similar UV–vis spectrum changes were observed by analysis of the AuNPs/MCH-gelatin. Zhao et al. [38] reported that MCH treatment affects the stability of modified AuNPs by reducing the number of substrate molecules on each AuNP. Therefore, the absorbance at 280 nm in AuNPs/MCH-gelatin was smaller than in AuNPs-gelatin. In Zhao et al.'s report [39], it was proposed that the uncharged MCH molecules themselves had little effect on colloidal stability.

The prepared AuNPs-gelatin and AuNPs/MCH-gelatin were treated with trypsin and then analyzed by UV–vis absorbance spectrophotometry, gel electrophoresis, and SEM. The absorbance spectra showed a decrease in the surface plasmon resonance at 280 nm when the AuNPs-gelatin were digested by trypsin (marked in blue in Fig. 1B), but no red shift or AuNPs aggregation was observed. In contrast, in the trypsin-digested AuNPs/MCH-gelatin, not only absorbance spectra decreases detected at 280 nm, but also the waveform of the AuNPs/MCH-gelatin broadened and a red shift was observed (marked in blue in Fig. 1C).

Jena and Raj [40] reported that the SPR band depends on the shape, size and distribution of the nanoparticles. From our results, the λ_{max} of AuNPs/MCH-gelatin was similar to that of AuNPs-gelatin, which hinted that the AuNPs-gelatin modification with MCH did not change the particle size. We can speculate that the MCH modification on AuNPs-gelatin can change the properties of the AuNPs-gelatin and induced the modified AuNPs to aggregate, while proteinase digests the gelatin on the AuNPs-gelatin. To confirm that the aggregation of AuNPs/MCH-gelatin is due to the gelatin being digested by proteinase, we used the proteinase inhibitors (A1AT for trypsin and ONO-4817 for MMP-2) to block either trypsin or MMP-2 activity in the detection. The result indicated that while the proteinase activity was inhibited by their inhibitors, the AuNPs/MCH-gelatin kept dispersion; otherwise AuNPs/MCH-gelatin would aggregate after proteinase digesting the substrate (data not shown). The result of activity inhibition of proteinase reveals that the

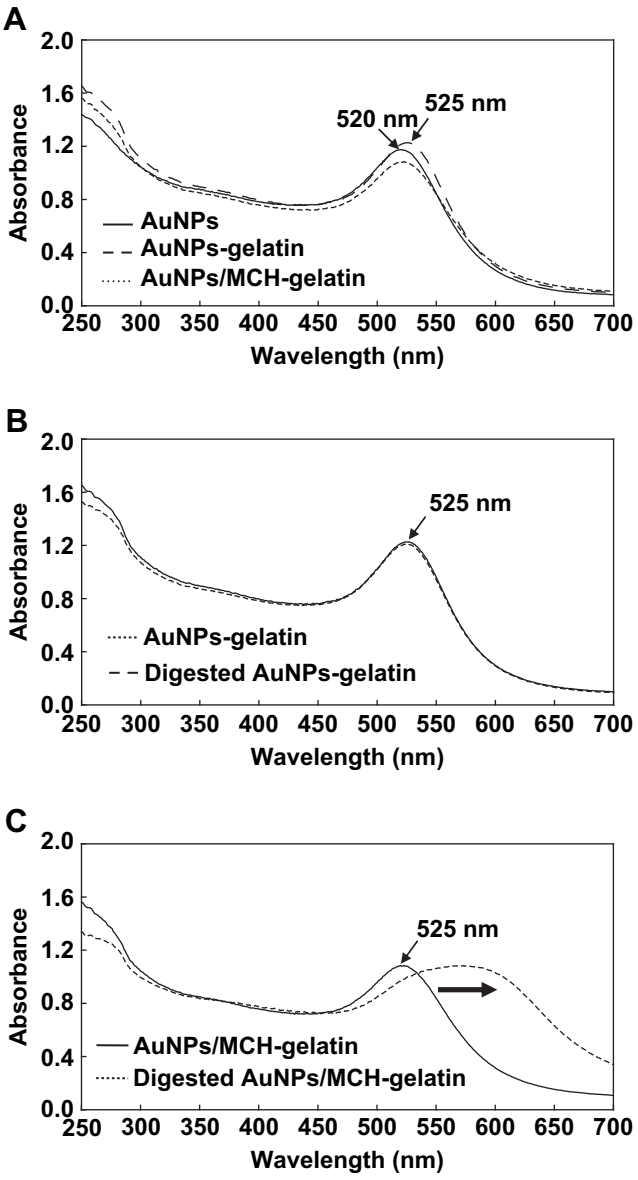

Fig. 1. UV–vis absorption spectra of gelatin-conjugated AuNPs treated with trypsin. (A) The red line represented the unmodified 13 nm AuNPs. The peak at 520 nm was due to plasmon resonance absorption of the bare 13 nm AuNPs. The blue line and black line represented the spectral profile of AuNPs-gelatin and AuNPs/MCH-gelatin, respectively. The SPR peak of the modified AuNPs was seen to shift slightly from 520 nm to 525 nm, and the appearance of the peak around 280 nm was due to absorption by the gelatin conjugated onto the AuNPs. In the sample of AuNPs-gelatin digested by trypsin, the absorbance at 525 nm showed no change and there was no significant red shift in peak position (B). In the sample of AuNPs/MCH-gelatin digested by trypsin, the absorbance at 525 nm decreased and the absorbance at 625 nm significantly increased (C).

aggregation of functionalized-AuNPs is due to proteinase digesting the gelatin that was modified onto AuNPs.

The ratios of A_{625}/A_{525} throughout the processes of AuNPs modification and proteinase digestion were also determined. The A_{625}/A_{525} ratio of AuNPs, AuNPs-gelatin and AuNPs/MCH-gelatin were 0.143 ± 0.002, 0.153 ± 0.001 and 0.194 ± 0.003 ($n = 3$), respectively. The both differences between AuNPs and AuNPs-gelatin, and AuNPs-gelatin and AuNPs/MCH-gelatin were statistically significant ($p < 0.01$ for AuNPs *vs.* AuNPs-gelatin and for AuNPs-gelatin *vs.* AuNPs/MCH-gelatin). Based on the changes in absorbance λ_{max} and the ratio of the modified AuNPs, the results indicate that MCH modification can affect the physical properties of AuNPs.

3.3. Characterization of modified AuNPs

The electrophoresis was used to identify the properties of the modified AuNPs according to the results of nanoparticle mobility in the electrophoretic gel. Because SDS absorbed on the modified AuNPs surface confers strong negative charges, all of the modified AuNPs retained negative charges, and the primary effect for electrophoretic mobility due to the size of the modified AuNPs, therefore, the electrophoretic mobility is direct surrogate for size [41,42]. In Fig. 2, the bare AuNPs showed the fastest mobility in the agarose gel, because the size of the bare AuNPs is the smallest compared with the modified AuNPs. Furthermore, for AuNPs-gelatin, the particle sizes decreased and were dependent on the enzyme activity. However, the sizes of the trypsin-digested AuNPs-gelatin were still larger than those of the bare ones, indicating that the trypsin did not completely cleave the gelatin on the AuNPs surface; a similar result has also been reported by [43]. In contrast to the results obtained from the AuNPs-gelatin, the AuNPs/MCH-gelatin were observed to aggregate after trypsin digestion, and therefore they moved with difficulty in the agarose gel and remained in the well (Fig. 2).

The proteinase treatment-induced aggregation of modified AuNPs was identified by SEM observations. The images shown in Fig. 3A–E confirm the size variation of modified AuNPs upon proteinase digestion. In the absence of proteinase, all of the AuNPs in this study remained dispersed (Fig. 3A–C). In the presence of proteinase, AuNPs-gelatin showed a slight aggregation (Fig. 3D), and AuNPs/MCH-gelatin displayed a predominant aggregation of nanoparticles (Fig. 3E).

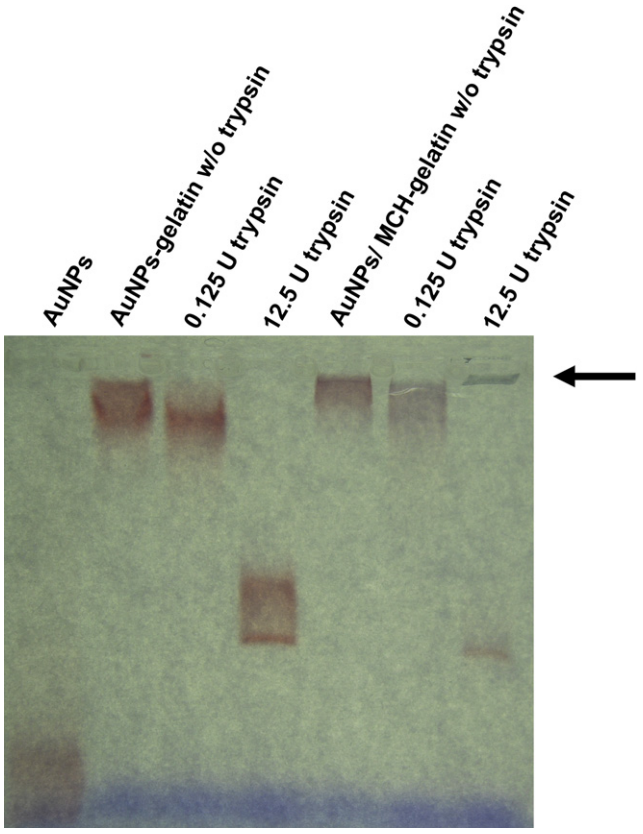

Fig. 2. Electrophoresis mobility of modified AuNPs. Electrophoretic separation of AuNPs was performed on a 0.5% agarose gel run for 30 min at 110 V in 0.5× TBE buffer, followed by staining with Coomassie brilliant blue. The bare AuNPs showed the fastest mobility in the agarose gel due to the small particle size of the bare AuNPs as compared with the modified AuNPs. The arrow indicates the aggregated AuNPs/MCH-gelatin that was digested by trypsin.

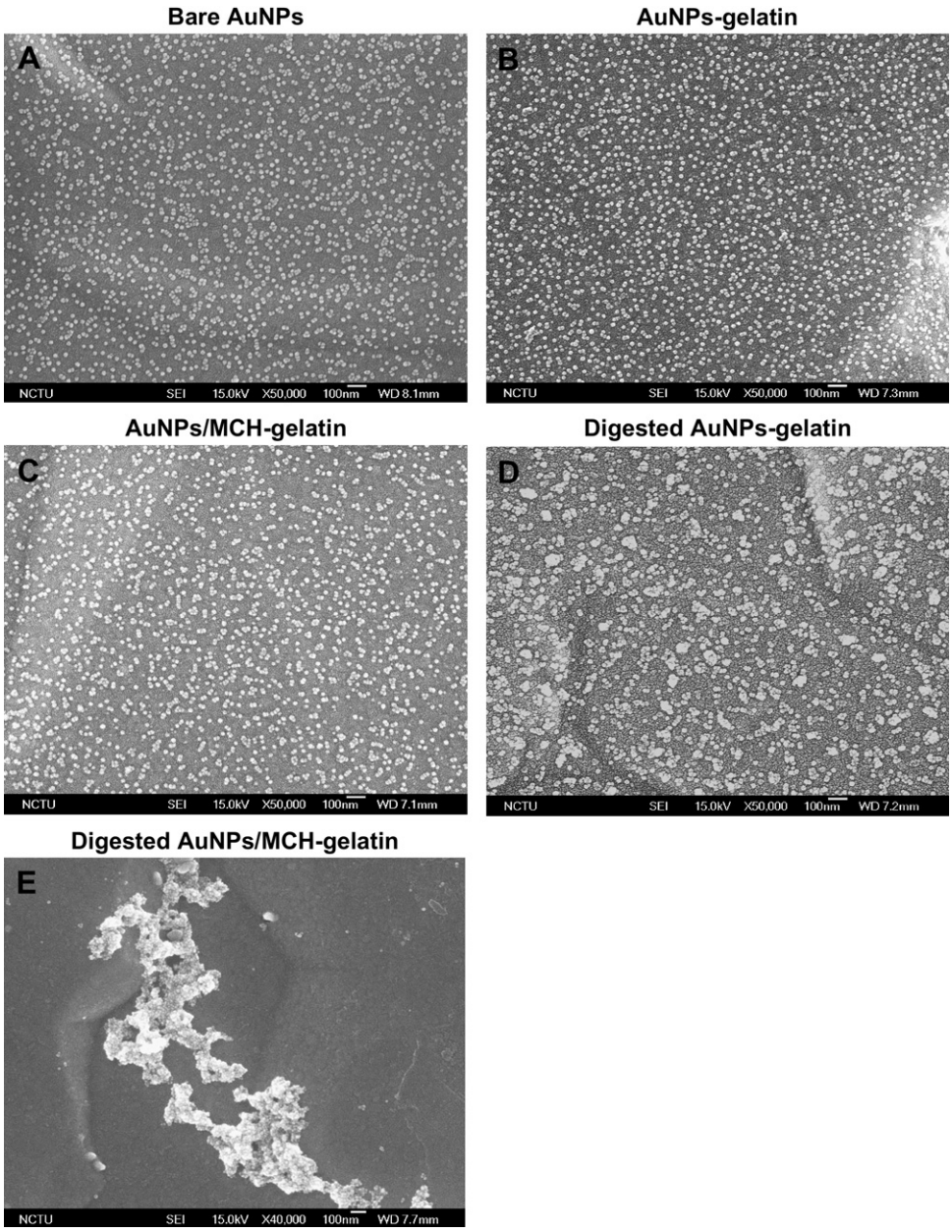

Fig. 3. Scanning electron microscope (SEM) image of modified AuNPs. The SEM images were observed from samples of bare AuNPs, AuNPs-gelatin and AuNPs/MCH-gelatin (A–C). The AuNPs-gelatin digested by trypsin remained monodispersed (D). The AuNPs/MCH-gelatin digested by trypsin showed aggregation and therefore moved with difficulty in the agarose gel, staying in the well of the electrophoretic gel (indicated by arrow) (E).

Dynamic light scattering (DLS) measurements were performed to determine the sizes and size population distributions of AuNPs. The determinations showed that gelatin modification was crucial for the size extension of AuNPs. The hydrodynamic diameters of AuNPs-gelatin increased to approximately 28 nm upon gelatin modification from the bare AuNPs with sizes around 13 nm (Fig. 4A and B). After MCH was immobilized on AuNPs-gelatin, the size of AuNPs/gelatin-MCH showed little variation compared to those of AuNPs-gelatin (Fig. 4C).

3.4. Colorimetric assay for proteinase by using AuNPs/MCH-gelatin

The colorimetric assay for proteinase activity using AuNPs/MCH-gelatin was carried out with determination by UV–vis spectroscopy. Trypsin at concentrations over the range of 1.25×10^{-2} U to 1.25×10^{2} U was used in this study to test the detection limits and the range of the optical AuNPs biosensing platform. The colorimetric response and the wavelength change were exhibited in Fig. 5A. The λ_{max} of AuNPs/MCH-gelatin was originally located at 525 nm, and upon trypsin digestion of the AuNPs/MCH-gelatin, the absorbance decreased at 525 nm without showing the red shift phenomenon. Additionally, the absorbance at the 625 nm wavelength rose when trypsin activity was increased. Furthermore, the color of the AuNPs/MCH-gelatin changed from wine-red to purple. We speculated that the decreasing absorbance at 525 nm was dependent on trypsin cleavage of the AuNPs/MCH-gelatin and caused the interparticle distances to decrease, while increasing the absorbance at 625 nm was dependent on the AuNPs aggregation. Our results demonstrated that the rate of color change in the developed colorimetric biosensing method was directly related to the amount of proteinase used in the assay. The method provides the possibility of quantitatively evaluating proteinase activity.

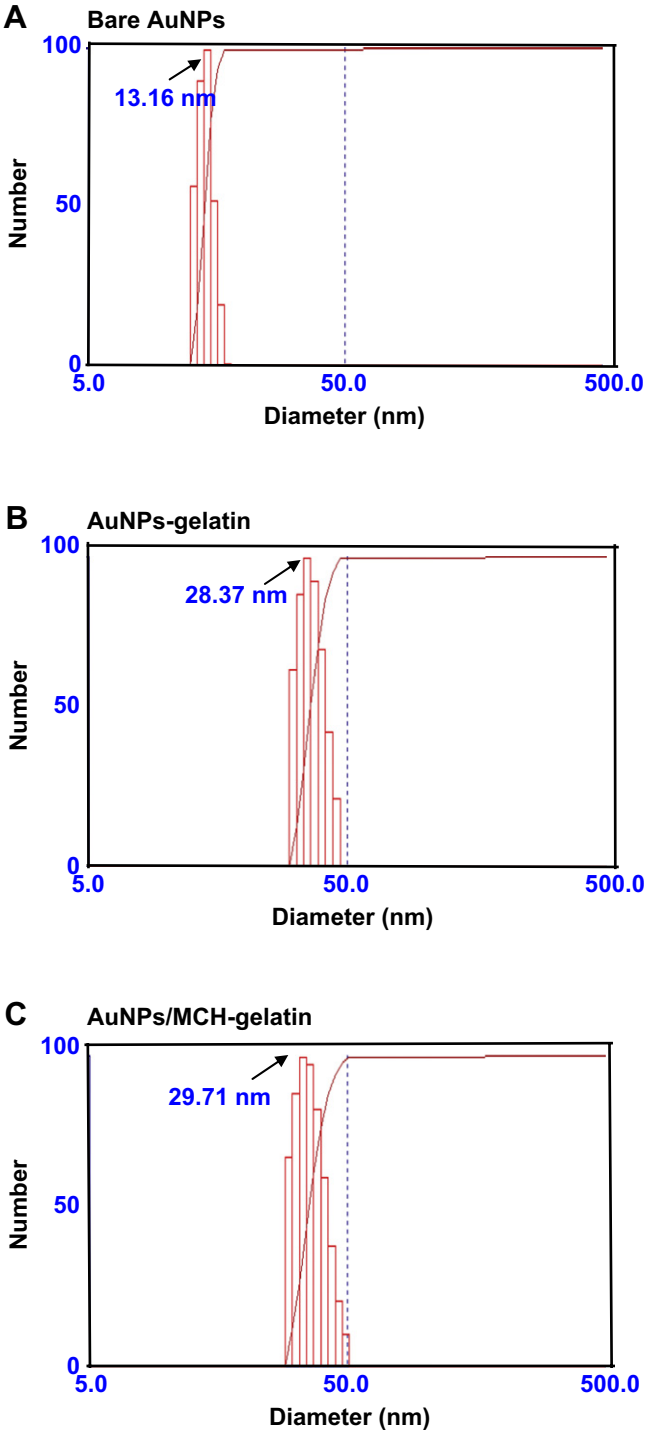

Fig. 4. Analysis of nanoparticle size by dynamic light scattering. Plots of size distribution of bare AuNPs (A), AuNPs-gelatin (B) and AuNPs/MCH-gelatin (C) are displayed.

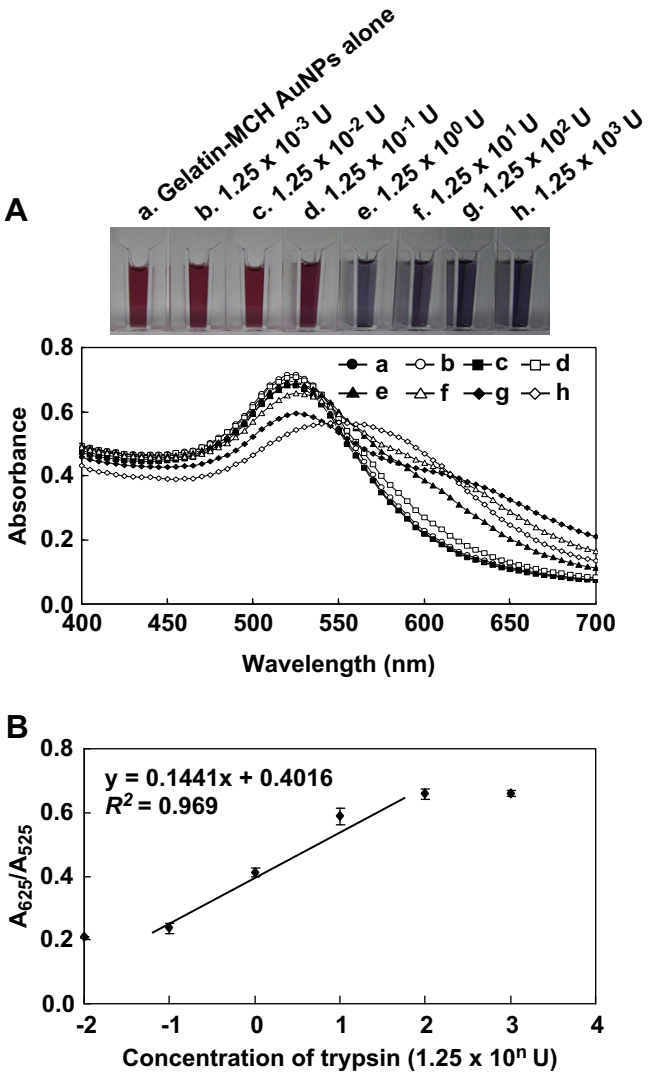

Fig. 5. Absorption spectra of AuNPs/MCH-gelatin in the presence of trypsin. Colorimetric assay of the AuNP/MCH-gelatin at 10 min after incubation with different concentrations of trypsin (A). (a) AuNPs/MCH-gelatin only; (b) to (h) different concentrations of trypsin added from 1.25×10^{-3} to 1.25×10^{3} U. When the AuNPs/MCH-gelatin was digested by trypsin, aggregation of AuNPs caused the λ_{max} at 525 nm to decrease, and a new λ_{max} emerged at 625 nm. The A_{625}/A_{525} ratios of AuNPs/MCH-gelatin calculated from UV–vis spectra recorded at 10 min were plotted as a function of the trypsin concentration. The correlation coefficients were 0.9572 (R^2) for the determination of trypsin activity in the concentration range from 1.25×10^{-1} to 1.25×10^{2} U (B). Each value represents mean ± standard deviation derived from three independent detections. Each value indicates mean ± standard deviation (S.D.).

When enzymes carry out their function, changing the reaction conditions, such as pH, temperature, metal ion or salt concentration, would affect the activity of enzymes. Accordingly, we have performed the experiments to explore the optimal condition of reaction. The effects of pH and NaCl concentration of NTTC buffer on the reaction of AuNPs aggregation were evaluated and the results showed that the optimized pH and NaCl concentration located at pH 8 and 100 mM of NaCl. This optimized pH value and salt concentration was close to those in physiological fluids; therefore, we used pH 7.5 (the normal serum pH is around 7.4) and 100 mM of NTTC as reaction buffer to analyze proteinase activity.

To quantify the proteinase activity, the ratios of spectral absorbance A_{625}/A_{525} at 10 min after trypsin digestion of the AuNPs/MCH-gelatin were plotted as a function of the trypsin concentration (Fig. 5B). These two absorbances, A_{625} and A_{525}, can be chosen to represent the relative amount of aggregated and suspended AuNPs, respectively [44]. Fig. 5B shows a plot of the value of A_{625}/A_{525} of the AuNP/MCH-gelatin against the concentration of trypsin (1.25×10^{-2} to 1.25×10^{2} U), and the linear relation can be found from 1.25×10^{-1} to 1.25×10^{2} U ($y = 0.1441x + 0.5457$, $R^2 = 0.969$). With the proteinase activity assay using the AuNPs-based method, the proteinase activity could be detected within a 10 min reaction time. The detection limit of the present method can decrease to

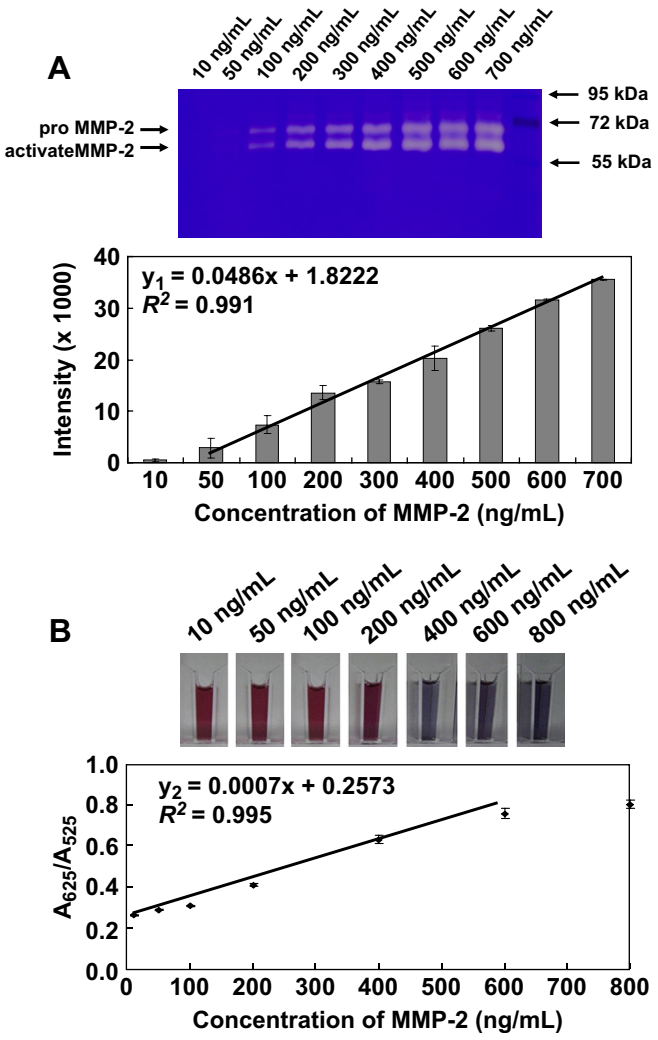

Fig. 6. MMP-2 activity assay by the methods of conventional zymography and optical AuNPs/MCH-gelatin. A representative assay using gelatin zymography showed pro-MMP-2 (latent form; 72 kDa) and active MMP-2 (68 kDa) detection, and a linear relationship was found between the intensity of image *vs*. MMP-2 from 50 ng/mL to 700 ng/mL (A). The colorimetric assay using AuNPs/MCH-gelatin was applied to determinate MMP-2 activity. Upon increasing the concentration of MMP-2, the value of A_{625}/A_{525} was increased. A linear correlation existed between the value of A_{625}/A_{525} and the concentration of MMP-2 over the concentration range of 20–600 ng/mL (B). Each bar or value indicates mean ± SD.

Table 1
Comparisons of the zymography assay and the AuNPs platform used to assay gelatinase activity.

	Zymography	AuNPs platform (AnNPs/MCH-gelatin)
Detection time	>16 h	30 min
Detection limit	50–700 ng/mL	20–600 ng/mL
Signal detection	By densitometric analysis[a]	By UV–vis spectrum
Diagnostic process	Three-step[b]	One-step
MMP typing	Yes	No (especially to distinguish the gelatinase activity come from MMP-2 and MMP-9)

[a] The zymography gels were scanned using Adobe Photoshop software (Adobe Systems, Inc., CA), and densitometric quantification using Image J was performed.
[b] Electrophoresis-reactive-imaging.

approximately 0.01 U of trypsin applied. Zhao et al. [39] reported that macromolecules grafted onto colloid surfaces provide steric stabilization and make the colloid much less sensitive towards ionic strength. Therefore, previous studies using macromolecules (such as antigen or human serum albumin) grafted onto colloid surfaces had a narrow detection range, and the dynamic range were one or two orders of magnitude [21,45,46]. Upon MCH treatment, our system had a broader detection range and the dynamic range is three orders of magnitude.

3.5. Activity assay of MMPs by zymography and AuNPs/MCH-gelatin

To demonstrate the activity of MMP-2, assays of in-gel gelatin zymography were performed. The representative gelatin zymography shown in Fig. 6A presented two predominant gelatinase activities migrating at 72 kDa and 68 kDa, corresponding to pro-MMP-2 (latent form) and MMP-2 (active form), respectively [5]. In the process of running the gel, the thiol-modifying reagent, SDS, can lead to MMPs activation *in vitro* [1]; therefore, the pro-MMP-2 displayed activity in the gel. The total zymographic activity of MMP-2 was quantified using densitometric analysis (Fig. 6A). The gelatinase activity of MMP-2 (including latent and active forms) increases with the amount of MMP-2, and the measurements were highly reproducible for all concentrations of MMP-2. For the detection by zymography, a linear relationship was found between the intensity of the image *vs*. MMP-2 over concentrations from 50 ng/mL to 700 ng/mL ($y_1 = 0.0486x + 1.1882$, $R^2 = 0.991$).

The same test was carried out by the developed colorimetric biosensing method using AuNPs/MCH-gelatin. As shown in Fig. 6B,

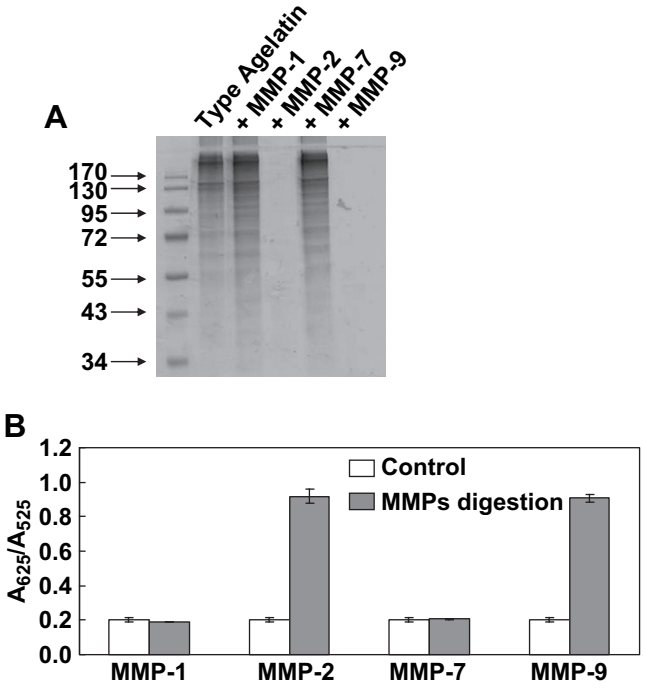

Fig. 7. Specificity of AuNPs/MCH-gelatin used in the detection of MMPs activity. MMPs, including MMP-1, MMP-2, MMP-7 and MMP-9, were used to test the specificity of the AuNPs/MCH-gelatin platform. Gelatin degradation by the MMPs treatment was monitored by 8% SDS-PAGE and Coomassie brilliant blue staining (A). Lane 1, gelatin alone; Lane 2, gelatin with MMP-2 treatment; Lane 3, gelatin with MMP-9 treatment; Lane 4, gelatin with MMP-1 treatment; and Lane 5, gelatin with MMP-7 treatment. The AuNP/MCH-gelatin was used to determine the MMPs activity, and the ratios of A_{625}/A_{525} were calculated before and after MMP-2, MMP-9, MMP-1 and MMP-7 treatment (B). Each bar indicates mean ± SD.

visualization of different solution colors were dependent on amount of MMP-2 over concentrations from 10 ng/mL to 800 ng/mL. Upon increasing the concentration of MMP-2, the value of A_{625}/A_{525} was increased. A linear correlation was shown to exist between the value of A_{625}/A_{525} and the concentration of MMP-2 over the range of 20–600 ng/mL ($R^2 = 0.995$).

We compared the advantages of the AuNPs platform and the zymography method used to detect MMP-2 activity in Table 1. The optical method established on the AuNPs was more rapid than the traditional zymography method (10 min *vs.* 16 h). Both methods could detect MMP-2 activity over a similar range. However, detection using the AuNPs platform can be carried out in only one step, and signal detection simply involves the direct measurement of the absorbance values obtained at A_{625} and A_{525}. Based on the advantages of the AuNPs platform used for the detection of proteinase activity, this method has the potential to be developed as a system for point-of-care biosensor. However, a major disadvantage of the developed AuNPs platform is that the method cannot be used to distinguish among gelatinase activity from different MMPs, especially MMP-2 (gelatinase A) and MMP-9 (gelatinase B) (Fig. 6A).

3.6. Specificity of AuNPs/MCH-gelatin used in the MMPs activity assay

To assess the selectivity of the AuNPs/MCH-gelatin towards proteinase, four MMPs (MMP-1, MMP-2, MMP-7, and MMP-9) were studied. In Fig. 7A, gelatin degradation by MMPs treatment was resolved on an 8% SDS-PAGE gel, and the major molecular masses of gelatin, as seen on the gel, were greater than 95 kDa. Under the assay conditions used, MMP-2 and MMP-9 completely degraded the gelatin, whereas only a slight degradation occurred when gelatin was treated with MMP-7 (Matrilysin 1) and MMP-1 (collagenase 1). These data were confirmed by a report from Snoek-van Beurden and Von den Hoff [47], who indicated that gelatin was the major substrate of MMP-2 but was a minor substrate of MMP-7; therefore, MMP-7 did not digest gelatin, and only a few gelatin fragments appeared at lower sites.

The MMPs were also used to test the enzyme specificity of the AuNPs/MCH-gelatin (Fig. 7B). The A_{625}/A_{525} ratio increased from 0.2 to 0.9 after MMP-2 or MMP-9 was applied to digest the gelatin on the AuNPs/MCH-gelatin. In contrast to the treatment by MMP-1 and MMP-7, the values of the A_{625}/A_{525} ratio were similar before and after enzyme treatment. Comparison of the AuNPs platform with the SDS-PAGE assay for gelatinase activity showed that the AuNPs platform began aggregation only when the gelatin was digested to small peptides. Accordingly, the AuNPs platform performed with more effective than the SDS-PAGE method for the gelatinase activity assay but did not differentiate between the activity arising from MMP-2 or MMP-9, two of the predominant gelatinases.

4. Conclusions

In the present study, we demonstrated a method of colorimetric proteinase assays by exploiting the color shift produced upon aggregation of functionalized-AuNPs. The aggregation of AuNPs changes their optical properties, i.e., their surface plasmon resonance, and this change can be detected by visualization in solution with the naked eye as the color changes from red to purple or through the use of UV–vis spectroscopy to quantify the proteinase activity. This established AuNPs-based biosensing platform is potentially applied as the diagnostic method for assay of proteinase activity, the proteinase activity could be determined within 10 min and the detection limit for trypsin is 1.25×10^{-2} U as well as for MMP-2 is 20 ng/mL.

Acknowledgments

This work was supported by grants NSC 95-2313-B-009-002-MY3 and NSC 96-2628-B-009-001-MY3 from the National Science Council of Taiwan. This work was also partially supported by the Ministry of Education under a grant from the MOE ATU Program, Taiwan. The authors thank Prof. Fu-Hsiang Ko, faculty at the Institute of Nanotechnology and Department of Materials Science and Engineering of National Chiao Tung University, for the supporting nanotechniques.

Appendix

Figures with essential colour discrimination. Figs. 2, 4–6 in this article may be difficult to interpret in black and white. The full colour images can be found in the on-line version, at doi:10.1016/j.biomaterials.2010.04.026.

References

[1] Folgueras AR, Pendás AM, Sánchez LM, López-Otín C. Matrix metalloproteinases in cancer: from new functions to improved inhibition strategies. Intd J Dev Biol 2004;48:411–24.
[2] Schulz R. Intracellular targets of matrix metalloproteinase-2 in cardiac disease: rationale and therapeutic approaches. Annu Rev Pharmacol 2007;47:211–42.
[3] Johnsen M, Lund LR, Rømer J, Almholt K, Danø K. Cancer invasion and tissue remodeling: common themes in proteolytic matrix degradation. Curr Opin Cell Biol 1998;10:667–71.
[4] Egeblad M, Werb Z. New functions for the matrix metalloproteinases in cancer progression. Nat Rev Cancer 2002;2:161–74.
[5] Chen CL, Huang SK, Lin JL, Lai LP, Lai SC, Liu CW, et al. Upregulation of matrix metalloproteinase-9 and tissue inhibitors of metalloproteinases in rapid atrial pacing-induced atrial fibrillation. J Mol Cell Cardiol 2008;45:742–53.
[6] Nath N, Chilkoti A. Label free colorimetric biosensing using nanoparticles. J Fluoresc 2004;14:377–89.
[7] Baptista P, Pereira E, Eaton P, Doria G, Miranda A, Gomes I, et al. Gold nanoparticles for the development of clinical diagnosis methods. Anal Bioanal Chem 2008;391:943–50.
[8] Chen SH, Wu VC, Chuang YC, Lin CS. Using oligonucleotide-functionalized Au nanoparticles to rapidly detect foodborne pathogens on a piezoelectric biosensor. J Microbiol Methods 2008;73:7–17.
[9] Rechberger W, Hohenau A, Leitner A, Krenn JR, Lamprecht B, Aussenegg FR. Optical properties of two interacting gold nanoparticles. Opt Commun 2003;220:137–41.
[10] Su KH, Wei QH, Zhang X, Mock JJ, Smith DR, Schultz S. Interparticle coupling effects on plasmon resonances of nanogold particles. Nano Lett 2003;3:1087–90.
[11] Wang C, Wang J, Liu D, Wang Z. Gold nanoparticle-based colorimetric sensor for studying the interactions of β-amyloid peptide with metallic ions. Talanta 2009;10:1016.
[12] Doria G, Franco R, Baptista P. Nanodiagnostics: fast colorimetric method for single nucleotide polymorphism/mutation detection. IET Nanobiotechnol 2007;1:53–7.
[13] Huang CC, Chiu SH, Huang YF, Chang HT. Aptamer-functionalized gold nanoparticles for turn-on light switch detection of platelet-derived growth factor. Anal Chem 2007;79:4798–804.
[14] Laromaine A, Koh L, Murugesan M, Ulijn RV, Stevens MM. Protease-triggered dispersion of nanoparticle assemblies. J Am Chem Soc 2007;129:4156–7.
[15] Medley CD, Smith JE, Tang Z, Wu Y, Bamrungsap S, Tan W. Gold nanoparticle-based colorimetric assay for the direct detection of cancerous cells. Anal Chem 2008;80:1067–72.
[16] Storhoff JJ, Lazarides AA, Mucic RC, Mirkin CA, Letsinger RL, Schatz GC. What controls the optical properties of DNA-linked gold nanoparticle assemblies? J Am Chem Soc 2000;122:4640–50.
[17] Jin R, Wu G, Li Z, Mirkin CA, Schatz GC. What controls the melting properties of DNA-linked gold nanoparticle assemblies? J Am Chem Soc 2003;125:1643–54.
[18] Sato K, Hosokawa K, Maeda M. Rapid aggregation of gold nanoparticles induced by non-cross-linking DNA hybridization. J Am Chem Soc 2003;125:8102–3.
[19] Thaxton CS, Georganopoulou DG, Mirkin CA. Gold nanoparticle probes for the detection of nucleic acid targets. Clin Chim Acta 2006;363:120–6.
[20] Shenton W, Davis SA, Mann S. Directed self-assembly of nanoparticles into macroscopic materials using antibody–antigen recognition. Adv Mater 1999;11:449–52.

[21] Thanh NTK, Rosenzweig Z. Development of an aggregation-based immunoassay for anti-protein a using gold nanoparticles. Anal Chem 2002;74:1624–8.
[22] Nam JM, Park SJ, Mirkin CA. Bio-barcodes based on oligonucleotide-modified nanoparticles. J Am Chem Soc 2002;124:3820–1.
[23] von Maltzahn G, Harris TJ, Park JH, Min DH, Schmidt AJ, Sailor MJ, et al. Nanoparticle self-assembly gated by logical proteolytic triggers. J Am Chem Soc 2007;129:6064–5.
[24] Chen SH, Lin KY, Tang CY, Peng SL, Chuang YC, Lin YR, et al. Optical detection of human papillomavirus type 16 and type 18 by the sequences sandwich hybridization with oligonucleotide-functionalized Au nanoparticles. IEEE T Nanobiosci 2009;8:120–31.
[25] Wang Z, Lévy R, Fernig DG, Brust M. Kinase-catalyzed modification of gold nanoparticles: a new approach to colorimetric kinase activity screening. J Am Chem Soc 2006;128:2214–5.
[26] Xu X, Han MS, Mirkin CA. A gold-nanoparticle-based real-time colorimetric screening method for endonuclease activity and inhibition. Angew Chem Int Edit 2007;46:3468–70.
[27] Walker HW, Grant SB. Coagulation and stabilization of colloidal particles by adsorbed DNA block copolymers: the role of polymer conformation. Langmuir 1996;12:3151–6.
[28] Glomm WR. Functionalized gold nanoparticles for applications in bionanotechnology. J Disper Sci Technol 2005;26:389–414.
[29] Persoons A, Verbiest T. An experimental study on the preparation of gold nanoparticles and their properties. Faculteit Wetenschappen Department Chemie Afdeling Moleculaire en nanomaterialen; 2006:34–6. Katholieke universiteit Leuven.
[30] Saraiva SM, de Oliveira JF. Control of particle size in the preparation of colloidal gold. J Disper Sci Technol 2002;23:837–45.
[31] Hanauer M, Pierrat S, Zins I, Lotz A, Sönnichsen C. Separation of nanoparticles by gel electrophoresis according to size and shape. Nano Lett 2007;7:2881–5.
[32] Surugau N, Urban PL. Electrophoretic methods for separation of nanoparticles. J Sep Sci 2009;11:1889–906.
[33] Liu J, Lu Y. A colorimetric lead biosensor using DNAzyme-directed assembly of gold nanoparticles. J Am Chem Soc 2003;125:6642–3.
[34] Elghanian R, Storhoff JJ, Mucic RC, Letsinger RL, Mirkin CA. Selective colorimetric detection of polynucleotides based on the distance-dependent optical properties of gold nanoparticles. Science 1997;277:1078–81.
[35] Liu Y, Liu Y, Mernaugh RL, Zeng X. Single chain fragment variable recombinant antibody functionalized gold nanoparticles for a highly sensitive colorimetric immunoassay. Biosens Bioelectron 2009;24:2853–7.
[36] Aili D, Selegård R, Baltzer L, Enander K, Liedberg B. Colorimetric protein sensing by controlled assembly of gold nanoparticles functionalized with synthetic receptors. Small 2009;5:2445–52.
[37] Pandana H, Aschenbach KH, Gomez RD. Systematic aptamer-gold nanoparticle colorimetry for protein detection: thrombin. IEEE Sens J 2008;8:661–6.
[38] Zhao W, Chiuman W, Lam JC, McManus SA, Chen W, Cui Y, et al. DNA aptamer folding on gold nanoparticles: from colloid chemistry to biosensors. J Am Chem Soc 2008;130:3610–8.
[39] Zhao W, Brook MA, Li Y. Design of gold nanoparticle-based colorimetric biosensing assays. Chembiochem 2008;9:2363–71.
[40] Jena BK, Raj CR. Optical sensing of biomedically important polyionic drugs using nano-sized gold particles. Biosens Bioelectron 2008;23:1285–90.
[41] Zanchet D, Micheel CM, Parak WJ, Gerion D, Alivisatos AP. Electrophoretic isolation of discrete Au nanocrystal/DNA conjugates. Nano Lett 2001; 1:32–5.
[42] Parak WJ, Pellegrino T, Micheel CM, Gerion D, Williams SC, Alivisatos AP. Conformation of oligonucleotides attached to gold nanocrystals probed by gel electrophoresis. Nano Lett 2003;3:33–6.
[43] Dobrovolskaia MA, Patri AK, Zheng J, Clogston JD, Ayub N, Aggarwal P, et al. Interaction of colloidal gold nanoparticles with human blood: effects on particle size and analysis of plasma protein binding profiles. Nanomedicine-Uk 2009;5:106–17.
[44] Huang CC, Huang YF, Cao Z, Tan W, Chang HT. Aptamer-modified gold nanoparticles for colorimetric determination of platelet-derived growth factors and their receptors. Anal Chem 2005;77:5735–41.
[45] Anfossi L, Baggiani C, Giovannoli C, Giraudi G. Homogeneous immunoassay based on gold nanoparticles and visible absorption detection. Anal Bioanal Chem 2009;394:507–12.
[46] Wang C, Chen Y, Wang T, Ma Z, Su Z. Biorecognition-driven self-assembly of gold nanorods: a rapid and sensitive approach toward antibody sensing. Chem Mater 2007;19:5809–11.
[47] Snoek-van Beurden PA, Von den Hoff JW. Zymographic techniques for the analysis of matrix metalloproteinases and their inhibitors. Biotechniques 2005;38:73–83.